Tsunamis with non-tectonic sources

Tony Waltham

Abstract: Tsunamis created by volcanoes or landslides are more numerous than those originating from earthquakes. A tsunami carried large boulders to elevations of 200 metres on the island of Santiago, in the Cape Verde archipelago; it was generated by lateral failure of a volcano on the adjacent island. Elsewhere, numerous destructive tsunamis have been created by volcano collapses or by large pyroclastic flows. In addition, many tsunamis have developed in seas and lakes due to large rockfalls and landslides unrelated to volcanoes.

Tsunamis have leapt into wider general perception since the two catastrophic events, around Sumatra in 2004, and then on the east coast of Japan in 2011. Both of those were classic tectonic tsunamis generated after the feather-edge of a continental plate had been dragged downwards by subduction of an oceanic plate. When friction on the thrust fault was overcome by accumulated stress, the overlying plate suddenly rebounded upwards, pushing up the ocean floor, generating a tsunami, and incidentally generating an earthquake. The effects were catastrophic (Waltham 2005; Mimura et al 2011). Less well known are non-tectonic tsunamis created by landslides and volcanoes.

The author claims no original research on these features; he merely found interest in some key sites that he visited, and thought that they deserved wider recognition within the East Midlands Geological Society and perhaps elsewhere.

Landslides, into or beneath bodies of water, are clearly a significant cause of tsunamis. Many of these are normal slope failures, though some are triggered by earthquakes. Volcanoes are the sources of another large group of tsunamis. Many of these were created by lateral or flank collapses of volcanoes, notably on mid-ocean volcanic islands, whereas others have been caused by major volcanic explosions, caldera collapses or very large pyroclastic flows on maritime volcanoes. All these add up to a frequency that is greater than that of the classic fault-generated tsunami. A number have been observed in historical times, and many older events are now being recognised by interpretation of exotic landforms. Some of the more spectacular sites are noted below.

Santiago, Cape Verde Islands, 73 ka

Lateral or flank collapses (i.e. total or partial failure of a sector) of volcanic islands gained recognition as widespread, and relatively normal, when huge spreads of landslide debris and slipped blocks were identified by seabed surveys around the Hawaiian islands, each of which is essentially a very large basaltic volcano (Moore 1964). Various ‘asymmetric calderas’ were then re-interpreted as the scars of giant landslides to add to the list of island volcanoes that had collapsed in the distant past, for example the Valle de Bove on the flanks of Mount Etna (Guest et al. 2003). Only later were signs of their consequent tsunamis recognised on some of the neighbouring coastlines.

Among the cluster of volcanic islands that form the archipelago of Cape Verde in the eastern Atlantic Ocean, the almost-circular island of Fogo is conspicuous by being a single stratovolcano. Rising 7000 m from the ocean floor, it has a diameter of about 25 km at sea level, with its summit at an altitude of 2700 m. The island’s conical profile is broken by the scar of a massive lateral collapse of its eastern flank (Worsley 2015). The surviving head scar is a cliff more than 900 m tall overlooking a bowl in which Pico de Fogo is a substantial volcano formed entirely since the time of the lateral collapse and with its summit already higher than the remnant arc of its ancestral host volcano (Fig. 1). The Pico is still active and last erupted in 2015 (Worsley 2015).

The collapse of Fogo has been dated to about 73,000 years ago (Ramalho et al. 2015). The failure appears to have involved about 110 km^3 of rock (Barrett et al.

Figure 1. *Fogo, in the Cape Verde Islands, seen from Santiago, with the profile of its pre-collapse edifice (known as Monte Amarelo) sketched in; a bank of fog lies along the Fogo coast.*

2020), and there is no evidence that it was other than a single, rapid event. It created a major tsunami that had maximum impact on the larger island of Santiago; this lies directly in front of the Fogo collapse, with 55 km of open water between the two islands (Fig. 2). Tsunami sediments have been recorded at various sites on the west coast of Santiago, directly facing Fogo, but none lies at elevations above about 15 m; it appears that erosion has removed all or most of what might have once existed.

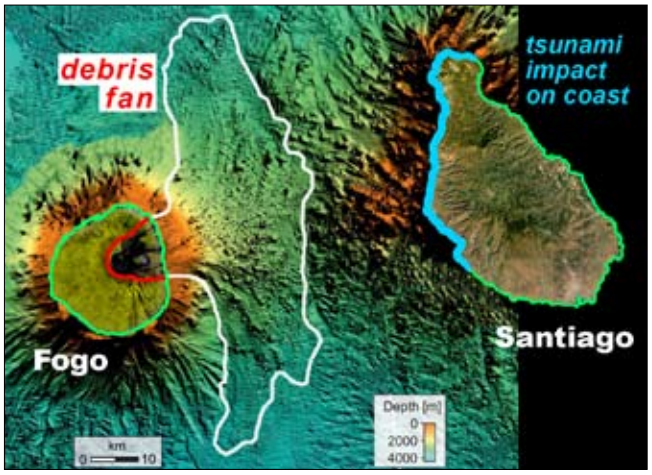

***Figure 2**. Fogo and Santiago, with an outline of the debris fan from Fogo's lateral collapse and the western part of the Santiago coast that was impacted by the tsunami (sea-bed data from Barrett et al. 2020).*

Truly spectacular are features on the north coast. More than 40 large boulders lie spread over the coastal plateau (Ramalho et al. 2015). The largest weighs about 700 tonnes (Fig. 3). Most are formed of submarine basalts and all can be recognised as being derived from outcrops at lower elevations. They have been moved up-slope to their present positions by the wash of a major tsunami. These boulders lie at elevations ranging between 160 and 220 m above present sea level. With mid-Devensian sea level about 60 m lower than at present, and an estimated 7 m of subsequent regional uplift, the boulders imply a tsunami run-up of at least 270 m, and this reached at least 650 m inland (Fig. 4).

Tsunami run-up is hugely influenced by coastal topography. The Santiago boulders lie around the heads of two steep valleys. Both of these are steep-sided, rock-walled valleys that taper inland to provide classic sites for a tsunami to grow in height where it is laterally confined (Fig. 5). Both valleys face northwest directly in line with the arrival of a Fogo tsunami that has been refracted around the northern end of Santiago. The boulders lie at optimum sites for tsunami run-up, but their elevations are still remarkable. Lateral collapse of the Fogo volcano appears to have generated a truly massive tsunami.

All the larger islands of Cape Verde show evidence of large flank landslides, though only Fogo and Santo Antao have failed in the last 400 ka. Continuing active

***Figure 3**. The largest of the tsunami boulders high above the north coast of Santiago island (the author failed to turn round beside the boulder before the camera's auto-timer fired).*

growth of Pico de Fogo raises the possibility of a repeat failure of the island's eastern flank; this could again create a large tsunami with potential impact on coastal sites, but prediction of the timing of such an event is impossible at present.

Lateral collapses of volcanoes are now recognised as major, frequent, and even normal features of large stratovolcanoes. The sheer scale of their debris avalanches can be massive, extending for many kilometres down adjacent valleys; that at Parinacota, though pre-historic, is a classic example and is still visually spectacular (Waltham 2004). Should such a debris mass encounter a lake, it can generate a very large tsunami. The eruption of Mt St Helens in 1980 was preceded by a massive lateral collapse; the debris avalanche from this ploughed upstream into Spirit Lake and pushed a tsunami to a height of 260 m at the head of its valley, though the effects of both were overshadowed by those of the lateral gas blast that arrived at almost the same time.

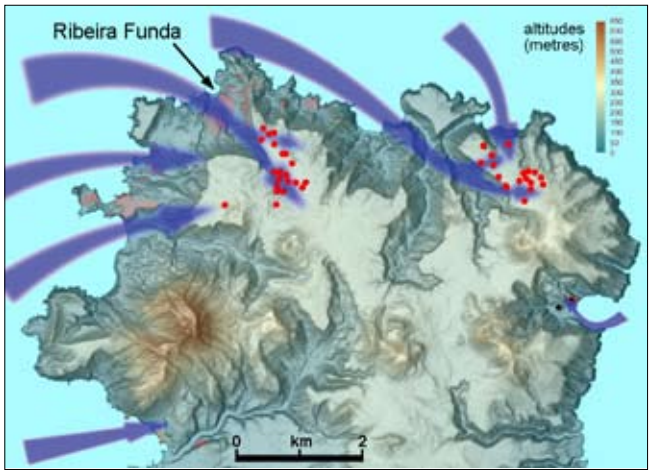

***Figure 4**. The northern end of Santiago; the pale area is the main plateau at altitudes above 150 metres. The blue arrows show the major wash-ups of the tsunami, and the red spots mark the known exotic blocks left by the tsunami (after Ramalho et al. 2015).*

***Figure 5**. The tapering valley of the Ribeira Funda, up which the tsunami rose carrying the large exotic blocks that are behind the camera position. The lines of vertical crags on both sides of the valley trace the outcrop of basaltic lavas that are identifiable as the source of the exotic blocks now lying at higher elevations than those outcrops.*

La Palma, Canary Islands

The western flank of La Palma bears the scars of two prehistoric lateral failures, from the Caldera de Taburiente (in this case, caldera is just the Spanish term for a deep bowl, and has no genetic implications) dated to about 530 ka, and the curved head scar of Cumbre Nueva, dated to around 520 ka (Fig. 6).

The southern ridge of the volcano, Cumbre Vieja, has a western slope of undeniable steepness and uncertain stability (Fig. 7). Open fissures near the crest of the slope were initially interpreted as head scars of a creeping block that could become a landslide up to 15 km wide and long (Ward & Day 2001). It was suggested that rapid failure of this could create a massive Atlantic tsunami, which was modelled to predict waves 25 m high along the American coast. This story was then picked up and blown out of all proportion by the press and media, which also invented disastrous tsunami impact on New York.

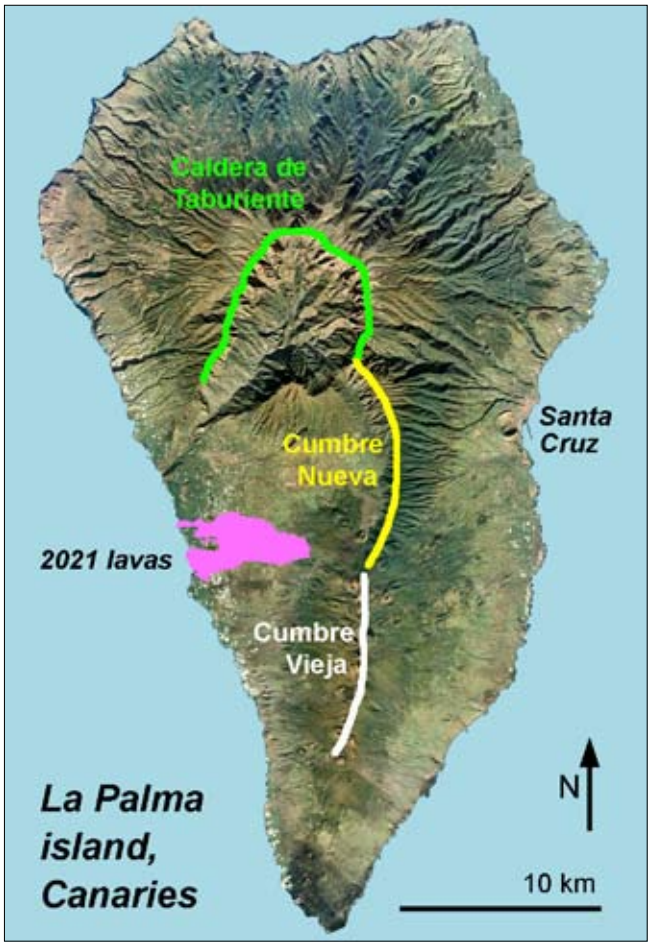

***Figure 6**. La Palma, Canary Islands, with the ancient landslide scars, recent lava flows and the potential head scar of a landslide on Cumbre Vieja.*

Subsequent fieldwork has revealed neither any instability of the hillside nor any further opening of the fissures at its head. The landslide potential is now relegated to remote, though is obviously not impossible. Furthermore, improved numerical modelling of tsunamis has indicated that even a worst-case scenario of a large, coherent and rapid slope failure on Cumbre Vieja would generate waves only a couple of metres high on the American coasts (HVO 2021).

The recent eruption on the flank of La Palma's volcano was north of the 'potential landslide' (Waltham 2023). This event could have improved slope stability with most of its lava accumulating on the lower parts of the slope and as a lava delta into the ocean, thereby increasing the toe weight, unless any potential slip

***Figure 7**. View along the steep western flank of Cumbre Vieja on La Palma, with the potential failure slope forming the distant skyline profile.*

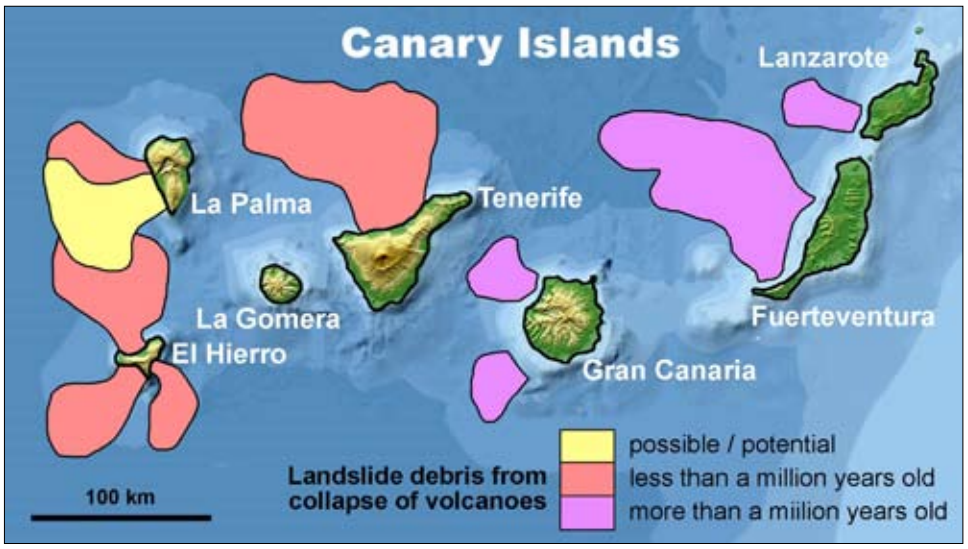

***Figure 8**. Submarine debris fans from lateral collapses of the volcanic Canary Islands (partly after Ward & Day 2001).*

surface extends far beneath sea level to intersect the lower, submarine profile of the volcano. The new eruption did re-awaken concerns over the potential landslide, but there is still no evidence for any correlation between eruptions and lateral collapses on these island volcanoes (Furst et al. 2023). The situation was not the same at Mt St Helens in 1980, when the rising magma initiated the landslide that caused the lateral component of the eruption blast (Waltham 1995); St Helens is an orogenic, andesitic volcano that is very different from a basaltic island volcano.

Lateral collapses of oceanic island volcanoes were first recognised on Hawaii, by their submarine fans of landslide debris (Moore 1964). Subsequently, debris fans have been found offshore from numerous other volcanic islands including all the Canary Islands except La Gomera (Fig. 8). The shape of Hierro is its own evidence of three lateral collapses radiating from its volcanic edifice. A massive debris fan extends across the seabed north of Tenerife (Watts & Masson 1995), confirming a giant landslide from the Teide volcano. However, controversy is still unresolved over genesis of the great asymmetrical basin of Las Canadas, on Teide, as to whether it is the surviving part of a caldera or is just the head scar of a giant landslide. All these Canary landslides are likely to have generated tsunamis on scales depending on the nature of the slope failures, either piecemeal or as single, rapid rockfalls; but they were long ago, and evidence of any consequent shoreline invasions has not yet been identified.

Tongatapu, Tonga

Isolated exotic boulders are known at two sites along the coasts of Tongatapu, the largest island in the Tonga archipelago. At Fahefa, on the west coast, the largest of these boulders is known as Tsunami Rock or Maui Rock (Fig. 9), with an estimated weight of more than 1500 tonnes. It lies at an elevation of 10 m, and is 130 m from the present shoreline. It consists of coral limestone, with dimensions that match a gap in the submarine reef just off-shore. At Haveluliku, near the western coast of Tongatapu, eight large coral boulders lie at elevations up to 30 m and as far as 500 m inland (Fig. 10). In addition, beds of distinctive, unsorted sediments have been recorded at other sites (Lavigne et al. 2021). The positions of the boulders and the sediments mean that they can only have been emplaced by one or more tsunamis, and organic material beneath them implies a date for their arrival in the mid-1400s.

Whereas the arrival of these boulders can be clearly assigned to a tsunami, the origin or cause of that tsunami remains open to debate. Numerical modelling of tsunamis that could reach the boulder sites, along

***Figure 9**. Tsunami Rock, 130 metres inland from the west coast of Tongatapu, Tonga.*

Figure 10. *Tongatapu, in the Tonga archipelago, with locations of recorded tsunami boulders.*

with assessment of historical records from the region, has proved inconclusive. Available evidence is against an earthquake source on the convergent boundary along the subducting western edge of the Pacific Plate, and caldera collapse of a volcano along the adjacent Tonga-Kermadoc island arc is perhaps the favoured origin (Lavigne et al. 2021).

A tsunami was generated nearby in 2022 by the violent volcanic eruption of Hunga Tonga–Hunga Ha'apai, which had formed a small island 70 km north of Tongatapu. This eruption was marked by the loudest explosion since that of Krakatau in 1883, sending air pressure waves around the world along with their coupled surface sea waves. Separate from those, tsunamis swept onto Tongatapu and many other Tongan islands, reaching elevations of 15 m as they travelled up to 500 m inland at some sites. Numerical modelling of the tsunamis indicates that they were formed by the caldera collapsing into the void created by the massive Surtseyan eruptions that destroyed the island (Lynett et al. 2022).

Krakatau, Indonesia, 1883

The eruption of Krakatau (commonly written as Krakatoa) on 27 August 1883 achieved lasting fame for the sound generated by its main explosion, and for the subsequent death toll of more than 36,000. Most of those people died in tsunamis that washed to altitudes of 30 to 40 metres on the heavily populated coastal regions of Sumatra and Java facing onto the Sunda Strait.

The air-pressure wave (effectively a burst of high wind) from the giant explosion did produce surface sea waves of significant size, but it appears that the infamous bang was not associated with any tsunami (i.e. a wave generated by seabed disturbance). Numerical modelling of the tsunami, correlated with wave height recordings along the nearby shores, indicate that the tsunami was created by a high-density pyroclastic flow, with a volume greater than 5 km^3, entering the sea at high speed (Maeno & Imamura 2011). The observed tsunami was not compatible with either a caldera collapse or a phreatomagmatic explosion, which were the alternative causes modelled and then rejected.

Perhaps in contrast, the 2018 eruption of Anak Krakatau (the younger volcano developed inside the 1883 caldera) generated a tsunami by sector collapse of its edifice during the opening stage of the event (Muhari et al. 2019). The nature of the collapse, whether mass sliding or blockfall, was unseen and remains unknown, but the resultant tsunami reached heights up to 13 m on nearby shores, where it caused the deaths of more than 400 people.

Santorini, Greece, 36ka

The Mediterranean volcanic island of Santorini (also known as Thera) has produced a series of massive eruptions and caldera collapses within the last 180,000 years (Fig. 11). Each of these likely produced major tsunamis, but the only one with its effects still recognisable was the last, widely known as the Minoan event a little more than 36,000 years ago. This eruption increased the depth of the northern part of the pre-existing caldera, which now contains the deepest water in between the islands that survive as fragments of the surrounding edifice. Both the volume of the submarine Minoan caldera and that of the eruption products on the adjacent sea floors exceed 30 km^3. The event caused, or at least contributed to, the demise of the Minoan civilisation; Akrotiri and other settlements on Santorini

Figure 11. *The smaller, western fragment of the Santorini volcano, Therasia, seen from the main island. The high cliff is part of the wall of the caldera, most of which is off to the left; the pale rock on the outer slope of the volcano is pumice from the Minoan eruption.*

were totally destroyed, and the eruption also impacted the island of Crete with tsunamis, earthquakes and airfall ash (Friedrich 2013). The scale of tsunami damage remains open to debate, but it appears that multiple tsunamis were produced, both by pyroclastic flows and by collapse of the caldera, and these probably washed to elevations of 20 or 30 metres on the northern coasts of Crete.

Lituya Bay, Alaska, 1958

A landslide into the head of this bay set into the southern coast of Alaska may still hold the record for the highest level reached by its resultant tsunami on 10 July 1958. The landslide originated from a height of around 900 m on the face of a glacially over-steepened rock wall above a narrow arm at the head of the T-shaped bay (Fig. 12). A slab of rock, 700 m wide and weighing in at more than 50 M tonnes, landed almost intact in the fjord just in front of the calving face of the Lituya Glacier. Displaced water was pushed straight ahead, across the fjord for nearly 1400 metres, and then up a forested slope on the opposite side (Fig. 13). There, mature spruce trees were destroyed to a maximum elevation of 524 m, at a distance of 1100 m from the shoreline (Miller 1960).

The crest of the wave was then deflected towards its left to pass over a shoulder within the hillside, to join the main bulk of the tsunami that rolled the length of Lityuya Bay. This part of the bay is around 3 km wide, but the tsunami left a trim line on both sides reaching 20 to 50 metres above tide level. At the mouth of the bay the wave, 12 km from its source, was still high enough to wash fishing boats at tree-top height over the sand spit that almost closes the bay.

Figure 12. *Lituya Bay, Alaska. The scar of the 1958 landslide is outlined in yellow, and the maximum height reached by the tsunami was on the far side of the ridge picked out in green; the wash line on this side of the ridge is picked out by the green dots, as far as its loss in the shadow of a cloud (photo: USGS).*

Figure 13. *Lituya Bay, with the wash line reached by the 1958 tsunami; the two opposing glaciers along the line of the Fairweather Fault appear grey due to their summer cover of moraine (base map from Google Earth, tsunami data after Moore 1960).*

The landslide had been triggered by an earthquake of M 8.3 created by movement on the Fairweather Fault (which has determined the shape of the bay, and was crossed by the run-out of the landslide). Fault displacement of about 7 m was almost horizontal, so there was no tectonic tsunami, and any seiche was subsumed by the landslide's tsunami.

Over-steepened slopes above water make fjord terrains especially susceptible to landslides and tsunamis. The higher and steeper slopes of Alaska and Norway are prime zones where there is the greatest hazard to their scatter of towns and villages. Lituya Bay has had five more landslide tsunamis recorded within the last 200 years, though none was as large as the 1958 event; the bay has no permanent population.

Greenland fjords

Greenland's spectacular fjords are also host to major landslides and tsunamis, with consequent hazard on the west coast where nearly all Greenlanders live. In June 2017, a large volume of rock broke away and fell 1000 m into Karrat Fjord. The tsunami reached more than 90 m high on the adjacent rock walls, washed 50 m high on the opposite wall of the 6 km-wide fjord, and destroyed much of the island village of Nuugaatsiaq (Schiermeier 2017). Subsequent fieldwork has revealed that another, even larger mass of rock is creeping forward high above Karrat Fjord, and three villages have been evacuated permanently in the face of the tsunami threat.

In July 2000, an estimated 30 M m^3 of rock fell away 1000 m above the fjord along the northern side of Disko Island (Pedersen et al. 2002). Its run-out over an alluvial fan reduced its impact on reaching the sea, so it was a smaller tsunami that caused modest damage in the village of Saqqaq some 40 km along the coast. This event was not unprecedented, and there is field evidence of multiple, prehistoric, even larger landslides and tsunamis in the same fjord (Korsgaard et al. 2023).

Tsunamis in the Greenland fjords would appear to be frequent events due to the normal processes of slope degradation.

Storegga, Norway, 8150 BP

The enormous submarine landslide at Storegga, off the coast of Norway in ~8150 BP, had multiple stages and was formed largely of poorly consolidated sediments that slumped off the edge of the continental shelf (Jansen et al. 1987). Slipped masses broke up to form debris flows that then disintegrated into turbidity flows, and consequently the event or events had less ability to generate tsunamis than do more intact landslide masses and rockfalls. Tsunami run-ups do not appear to have exceeded 25 m on the east coast of Shetland, and reached only about 5 m on the Scottish mainland (Smith et al. 2004). Any Storegga tsunami would have had major impact on low-level Doggerland, still then surviving in the southern North Sea, but it appears that most of the population had already left their watery homeland in the face of post-glacial rising sea level (Walker et al. 2020).

Tafjord, Norway, 1934

The steepness of the rock walls along glaciated troughs within Norway's fjordlands mean that rockfalls are a major component of their inevitable slope degradation. With many of the falls descending straight into deep water, tsunamis are therefore not infrequent on the fjords.

On 7 April 1934, the northern wall of Tafjord failed with about 4 M tonnes of rock falling the best part of 900 m down the very steep slope and directly into the fjord (Fig. 14). The resultant tsunami reached 62 m high on the adjacent cliffs and 37 m high on the equally steep rock wall a kilometre away on the opposite side of the fjord (Waltham 2002). The tsunami was sadly more destructive where it reached villages at both ends of the fiord; it reached 16 m up into the shore-side houses of Tafjord village, at the head of the fjord some 5 km from the rockfall source (Fig. 14). Movement on the rock face had been observed prior to 1934, but the subsequent failure was larger than expected.

Just 60 km south of Tafjord, progressive failure of a 1000-m-high cliff above Lake Loen created three major rockfalls in 1905, 1936 and 1950 (Waltham 2002). The first two events wrought massive destruction in lake-side villages, and the tsunami washed to a height of 74 m in 1936; the1950 rockfall created no tsunami simply because it landed on the previous debris so that most of it did not reach the lake.

The tsunami threat in Norway continues to this day. Located between Tafjord and Loen, an entire hillside is on the move at Aknes, directly above the deep waters of Sunnylvsfjord, which forms the approach to the well-known Geirangerfjord. A slab of gneiss, 30 m thick and totalling nearly 50 M m^3, is sliding on foliation that dips at around 35° towards the fjord (Fig. 15). The open and fresh fissure at the head of the slide, 900 m above fjord level, has been known since the 1960s. Subsequently movement of the entire slide has been seen to average 60 mm annually, and sometimes exceeds 1 mm per day.

Figure 15. *The creeping hillside above the fjord at Aknes, Norway. The fissure at the head of the moving slab is marked in red; the entrance to Geirangerfjord is almost directly behind the camera.*

Prediction of landslide movement is extremely difficult, and the worst-case scenario, with the whole mass at Aknes sliding rapidly into the fjord, could create a major tsunami. Since 2005, the site has been heavily monitored, with continuous laser scanning from across the fjord, in addition to arrays of extensometers,

Figure 14. *Tafjord, Norway. The pale scar beneath the red arrow is the site of the 1934 rockfall. The foreground buildings along the foreshore of Tafjord village are new boat houses, whereas the villagers now live at higher level behind the camera; houses along the foreshore were destroyed by the tsunami.*

inclinometers, peizometers and geophones. There are then links to warning systems in Hellesylt and Geiranger, small towns that lie at the heads of separate arms of the fjord and would both be impacted by a tsunami that could reach significant size.

Vaiont, Italy, 1963

The landslide in northern Italy that descended into the Vaiont Reservoir in 1963 created a tsunami that killed more than 2000 people (Fig. 16). Nearly all the extensive literature on the event cites the re-activation of an ancient landslide (Kiersch 1964; Genevois & Ghirotti 2005). However this concept was based on fieldwork carried out immediately after the event, perhaps rather hurriedly, and the site has since been re-assessed as a primary failure of steeply dipping limestones that contain weak shale beds (Dykes & Bromhead 2018). In both past and present concepts, the landslide trigger is recognised as a combination of prior heavy rainfall and the just-previous raising of ground pore-water pressures by the first filling of the reservoir. Vaiont still rates as the world's worst catastrophe caused by civil engineering works. The Vaiont Dam, with its tall, thin, cupola profile, was a masterpiece, but the selected site for the reservoir was a disaster.

After months of slow creeping, the landslide evolved into a rapid failure late in the night of 9 October 1963. Some 270 M m^3 of limestone slipped rapidly downhill, virtually as an intact mass, and fell into water more than 200 m deep. The tsunami wave swept more than 200 m up the opposite slope, less than 500 m away across the reservoir (Fig. 17). Fortunately the water did not reach the village of Casso, but two farm buildings at the lower end of the village were damaged by the air pressure wave ahead of the water wave.

The tsunami then washed both ways along the length of the reservoir. Most significantly, it was still more than 200 m tall where it overtopped the dam and dropped 250 m into the Viaont gorge. Compressed into the depths of this narrow ravine (Fig. 18), the wall of water was still more than 70 m tall when it exploded out into the Piave Valley, where it instantly destroyed most of the town of Longarone. The dam survived almost unscathed, even though the impact of the tsunami was greater than anything it had been designed to survive.

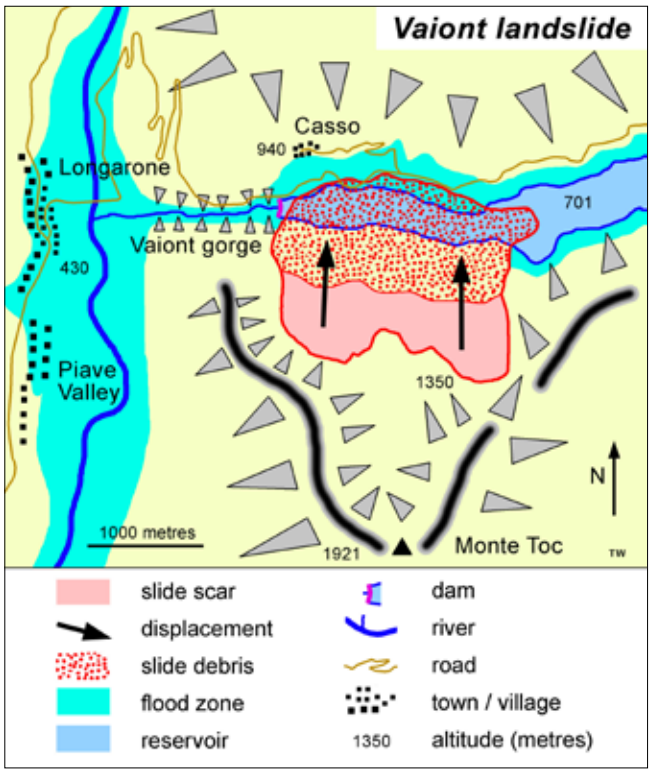

***Figure 17**. Main features of the Vaiont reservoir, landslide and tsunami.*

Landslides form a major part of the spectrum of slope failure processes within mountain terrains, and there are numerous cases of large masses of rock falling into lakes to create tsunamis that destroy shoreline villages. It is inevitable that more will occur in the future, but it is hoped that there will never again be a disaster created by the works of mankind, as was that at Vaiont.

***Figure 16**. The Vaiont landslide, Italy, seen from above the village of Casso in 2005. Bare limestone bedding planes identify the source of the slipped mass; the slide debris, completely filling this part of the reservoir, and with a cover of trees, forms all the ground beyond the spire of Casso church.*

***Figure 18**. The crest of Vaiont Dam seen from the road high in the downstream gorge in 1978. The projecting steel bars on the right are the remains of crash barriers destroyed by the tsunami; they are 250 metres above the floor of the gorge. The ridge on the right, beyond the dam, is the pile of landslide debris, prior to gaining much of its plant cover.*

Meteorite impacts

There is as yet no observation of a meteorite landing in water to create a tsunami. The effects of the Chicxulub meteorite that landed on the coast of Mexico at about 67 Ma have been modelled numerically, and indicate a tsunami approaching most coastlines of the North Atlantic and South Pacific (this was long before closure of the Panama Seaway) with waves more than 10 m high (Range et al. 2022). Such a tsunami would have been greater within the Gulf of Mexico, but its effects would have been subsumed by those of the explosion on impact.

It is notable that the Chicxulub tsunami modelling is keyed to shallow water at the point of impact. Any meteorite of comparable size would create a much larger tsunami if it landed in mid-ocean, where more of the impact energy would go into the water and not be taken by explosion of rock. Such a tsunami would have massive impact on coastlines of its host ocean, and would hardly be trivial all around the world.

With the statistical likelihood that any future meteorite will land in the dominating area of the world's oceans, its tsunami could well be its most destructive element. Fortunately, this will be a rare event, whereas landslides and volcanoes will continue to generate tsunamis of smaller size far more frequently.

References

The only papers cited are those freely available on-line; papers by the author can be downloaded from www.geophotos.co.uk/geology

Barrett, R. and 8 others, 2020. Revisiting the tsunamigenic volcanic flank collapse of Fogo Island in the Cape Verdes, offshore West Africa. *Geological Society Special Publication*, 500, 13–26, doi.org/10.1144/SP500-2019-187

Dykes, A.P. & Bromhead, E.N., 2018. The Vaiont landslide: re-assessment of the evidence leads to rejection of the consensus. *Landslides*, **15**, 1815–1832, doi:10.1007/s10346-018-0996-y

Friedrich, W.L., 2013. The Minoan eruption of Santorini around 1613 BC and its consequences. *Tagungen des Landesmuseums für Vorgeschichte Halle*, **9**, 37–48.

Furst, S., Urlaub, M., Klein, E. & Bonanati, C., 2023. Are eruptions reliable precursors to marine volcano collapses? *Frontiers in Earth Science*, **11**, doi:10.3389/feart.2023.1130561

Genevois, R. & Ghirotti, M., 2005. The 1963 Vaiont landslide. *Giornale di Geologia Applicata*, **1**, 41 –52, doi:10.1474/GGA.2005-01.0-05.0005

Guest, J.E., Cole, P.D., Duncan A.M. & Chester, D.K., 2003. *Volcanoes of southern Italy*. Geological Society: London, 284pp.

HVO (Hawaiian Volcano Observatory), 2021. The Canary Islands "mega-tsunami" hypothesis, and why it doesn't carry water. www.usgs.gov/observatories/hvo/news/

Jansen, E. and 5 others, 1987. Large submarine slides on the Norwegian continental margin. *Marine Geology*, **78**, 77–107.

Kiersch, G.A., 1964. Vaiont reservoir disaster. *Civil Engineering* (American Society of Civil Engineers), **60** (3), 32–39.

Korsgaard, N.J. and 5 others, 2023. Giant mid-Holocene landslide-generated tsunamis recorded in lake sediments from Saqqaq, West Greenland, *Natural Hazards Earth Systems Science*, doi:org/10.5194/nhess-2023-32

Lavigne F. and 17 others, 2021. Bridging legends and science: field evidence of a large tsunami that affected the Kingdom of Tonga in the 15th Century. *Frontiers in Earth Science,* **9**, doi:10.3389/feart.2021.748755

Lynett, P. and 17 others, 2022. Diverse tsunami genesis triggered by the Hunga Tonga-Hunga Ha'apai eruption. *Nature*, **609**, 728–733, doi.org/10.1038/s41586-022-05170-6

Maeno, F. & F. Imamura, 2011. Tsunami generation by a rapid entrance of pyroclastic flow into the sea during the 1883 Krakatau eruption, Indonesia, *Journal of Geophysical Research*, **116**, B09205, doi:10.1029/2011JB008253

Miller , D.J., 1960., Giant waves in Lituya Bay, Alaska. *U. S. Geological Survey Professional Paper*, 354-C, 49–87.

Mimura, N. and 4 others, 2011. Damage from the Great East Japan Earthquake and tsunami: a quick report. *Mitigation and Adaptation Strategies for Global Change*, **16**, 803-818, doi:10.1007/s11027-011-9297-7

Moore, J.G., 1964. Giant submarine landslides on the Hawaiian ridge. *U. S. Geological Survey Professional Paper*, 501-D, 95–98.

Muhari, A. and 8 others, 2019. The December 2018 Anak Krakatau volcano tsunami as inferred from post-tsunami field surveys and spectral analysis. *Pure and Applied Geophysics*, **176**, 5219–5233, doi:10.1007/s00024-019-02358-2

Pedersen, S. and 8 others, 2002. Tsunami-generating rock fall and landslide on the south coast of Nuussuaq, central West Greenland. *Geology of Greenland Survey Bulletin*, **191**, 73–93. doi.org/10.34194/ggub.v191.5131

Ramalho, R.S. and 7 others, 2015. Hazard potential of volcanic flank collapses raised by new megatsunami evidence. *Science Advances*, **1** (9), doi:10.1126/sciadv.1500456

Range, M.M. and 10 others, 2022. The Chicxulub impact produced a powerful global tsunami. *AGU Advances*, **3**, e2021AV000627, doi:org/10.1029/2021AV000627

Schiermeier, Q, 2017. Huge landslide triggered rare Greenland megatsunami. *Nature*, doi:10.1038/nature.2017.22374

Smith. D.E. and 10 ohers, 2004. The Holocene Storegga Slide tsunami in the United Kingdom. *Quaternary Science Reviews*, **23**, 2291–2321, doi:10.1016/j.quascirev.2004.04.001

Walker, J. and 6 others, 2020. A great wave: the Storegga tsunami and the end of Doggerland? *Antiquity*, **94**, 1409–1425.

Waltham, T., 1995. Excursion guide 11: Mt St Helens. *Geology Today*, **11**, 228–232.

Waltham, T., 2002. Unloading joints and rockfalls in Norway's fiordlands. *Geology Today*, **18**, 220–225.

Waltham, T., 2004. Parinacota, Chile. *Mercian Geologist*, **16**, 53.

Waltham, T., 2005. The Asian tsunami disaster, 2004. *Mercian Geologist*, **16**, 99–106.

Waltham, T., 2022. Atlantic volcanoes in action. *Mercian Geologist*, **20**, 200–207.

Ward, S.N. & Day, S., 2001. Cumbre Vieja volcano: potential collapse and tsunami at La Palma, Canary Islands. *Geophysical Research Letters*, **28**, 3397–3400.

Watts, A.B. & Masson, D.G., 1995. A giant landslide on the north flank of Tenerife, Canary Islands, *Journal of Geophysical Research*, **100**, 24,487–22,298.

Worsley, P., 2015. The 2014-15 volcanic eruption on Fogo, Cape Verde Islands. *Mercian Geologist*, **18**, 243–251.

Tony Waltham
11 Selby Road, Nottingham NG2 7BP
tony@geophotos.co.uk